ARMY RESEARCH LABORATORY

Multiscale Modeling of Non-crystalline Ceramics (Glass)

by George A. Gazonas, James W. McCauley, Iskander G. Batyrev, Richard C. Becker, Parimal Patel, Betsy M. Rice, and N. Scott Weingarten

ARL-MR-0765 **February 2011**

NOTICES

Disclaimers

The findings in this report are not to be construed as an official Department of the Army position unless so designated by other authorized documents.

Citation of manufacturer's or trade names does not constitute an official endorsement or approval of the use thereof.

Destroy this report when it is no longer needed. Do not return it to the originator.

Army Research Laboratory

Aberdeen Proving Ground, MD 21005-5066

ARL-MR-0765 **February 2011**

Multiscale Modeling of Non-crystalline Ceramics (Glass)

George A. Gazonas, James W. McCauley, Iskander G. Batyrev, Richard C. Becker, Parimal Patel, Betsy M. Rice, and N. Scott Weingarten

Weapons and Materials Research Directorate, ARL

REPORT DOCUMENTATION PAGE

Form Approved
OMB No. 0704-0188

1. REPORT DATE *(DD-MM-YYYY)*	2. REPORT TYPE	3. DATES COVERED (From - To)
February 2011	Progress	June 2010-October 2010

4. TITLE AND SUBTITLE
Multiscale Modeling of Non-crystalline Ceramics (Glass)

5a. CONTRACT NUMBER

5b. GRANT NUMBER

5c. PROGRAM ELEMENT NUMBER

6. AUTHOR(S)
George A. Gazonas, James W. McCauley, Iskander G. Batyrev, Richard C. Becker, Parimal Patel, Betsy M. Rice, N. Scott Weingarten

5d. PROJECT NUMBER
AH84

5e. TASK NUMBER

5f. WORK UNIT NUMBER

7. PERFORMING ORGANIZATION NAME(S) AND ADDRESS(ES)
U.S. Army Research Laboratory
ATTN: RDRL-WMM-B
Aberdeen Proving Ground, MD 21005-5069

8. PERFORMING ORGANIZATION REPORT NUMBER
ARL-MR-0765

9. SPONSORING/MONITORING AGENCY NAME(S) AND ADDRESS(ES)

10. SPONSOR/MONITOR'S ACRONYM(S)

11. SPONSOR/MONITOR'S REPORT NUMBER(S)

12. DISTRIBUTION/AVAILABILITY STATEMENT
Approved for public release; distribution is unlimited.

13. SUPPLEMENTARY NOTES
primary author's email: <george.aristotle.gazonas@us.army.mil>

14. ABSTRACT
This six-month progress report describes an ongoing program on the multiscale modeling of noncrystalline ceramics (glass) funded from the Director's Strategic Initiatives (DSIs) in support of the U.S. Army Research Laboratory's (ARL) Strategic Research Initiatives. The long-term research goal of the program is to develop a concurrent multiscale computational finite element code for optimizing or enhancing the performance of various glasses against shaped-charge jets; the initial work focuses on pure fused-silica (a-SiO_2), and chemically varied a-SiO_2 materials. As such, this objective falls squarely within the purview of the Weapons and Materials Research Directorate, since multiscale models are constitutive models (specific to a particular material) wherein time evolving short and intermediate range atomic structure, order, and microcrack initiation and growth, are fully coupled to the macroscale, a phenomenon that cannot be modeled or accounted for using classical homogenization methods. A more immediate research objective is to understand why certain chemically substituted a-SiO_2 materials exhibit enhanced performance in the defeat of shaped-charge jets and other ballistic threats.

15. SUBJECT TERMS
multiscale modeling; fused silica; amorphous quartz; molecular dynamics; quantum mechanics; shaped charge jet

16. SECURITY CLASSIFICATION OF:			17. LIMITATION OF ABSTRACT	18. NUMBER OF PAGES	19a. NAME OF RESPONSIBLE PERSON
a. REPORT	b. ABSTRACT	c. THIS PAGE			George A. Gazonas
Unclassified	Unclassified	Unclassified	UU	38	19b. TELEPHONE NUMBER (*Include area code*) 410-306-0863

Contents

List of Figures

INTENTIONALLY LEFT BLANK.

1. Introduction

Non-crystalline (amorphous) ceramics or ceramic glasses are used in a variety of vital Army personnel, ground, and air vehicle applications that require transparent armor − it is ubiquitous in tactical vehicular windshields and side windows. Ceramic glass is inexpensive and is formable into large, flat plate and curved shapes. For many years it has been known that the properties of glass can be modified and enhanced through compositional modification, chemical strengthening, annealing, and process control of melt cooling. Glass ceramics, the controlled crystallization of nano-sized single crystals in a glass matrix, offer another avenue for designed and enhanced property modifications for transparent and opaque material applications. In addition, certain glass formulations have been shown to exhibit enhanced performance against shaped-charge jets (SCJs) (figure 1) and other ballistic threats, but it is not understood why. This is in part due to various short and longer range atomic structural characteristics including atomic free volumes, cation coordinations, bridging and non-bridging oxygen (O) atoms, bonding energies, and nanoscale order characteristics (short and longer range) that are difficult or impossible to quantify experimentally for ceramic glass. In contrast, crystalline ceramics like silicon carbide (SiC), aluminum oxynitride ($AlON$), and others have easily characterizable microstructures/mesostructures, which consist of assemblies of individual single-crystal grains. Ceramic glasses, on the other hand, do not have a conventional micro- or mesostructure, as it is understood for crystalline ceramics. However, there are microstructural scale variations in ceramic glass that may include density variations from atomic free volume variations or microporosity, size of local atomic order, defects (inclusions, large pores, etc.), and others yet to be determined. The interaction of a stress/shock wave from a dynamic impact involves many structural changes not easily characterized by conventional equations of state and can involve reversible and irreversible densification and changes in bulk short range order structures comparable to phase changes in crystalline ceramics. For example, in simple Hertzian indentation testing, a wide range of plastic or inelastic deformation mechanisms have been observed in a variety of glasses. Multiscale computational design methodologies (figure 2), for this class of materials will, nevertheless, require quantitative and possibly statistically based descriptions of the mesoscale, although current efforts to develop such models have fallen far short of this goal.

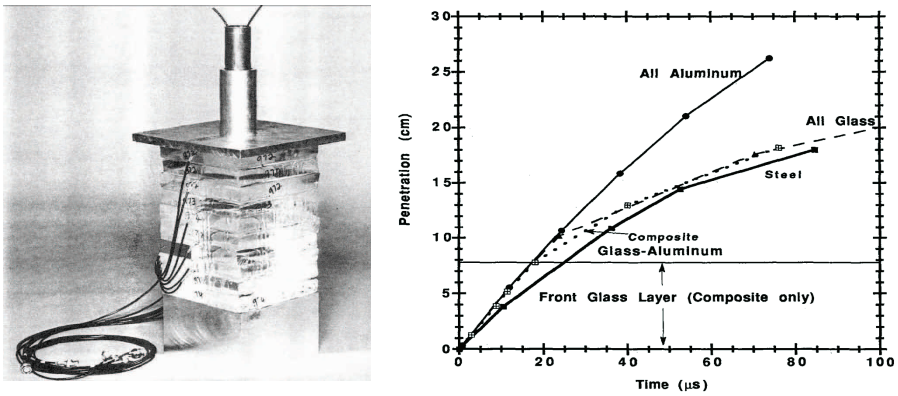

(a) (b)

Figure 1. Enhanced performance of SCJs into glass (a) test configuration for glass targets, and (b) penetration versus time for several targets, after Moran et al. (*1*).

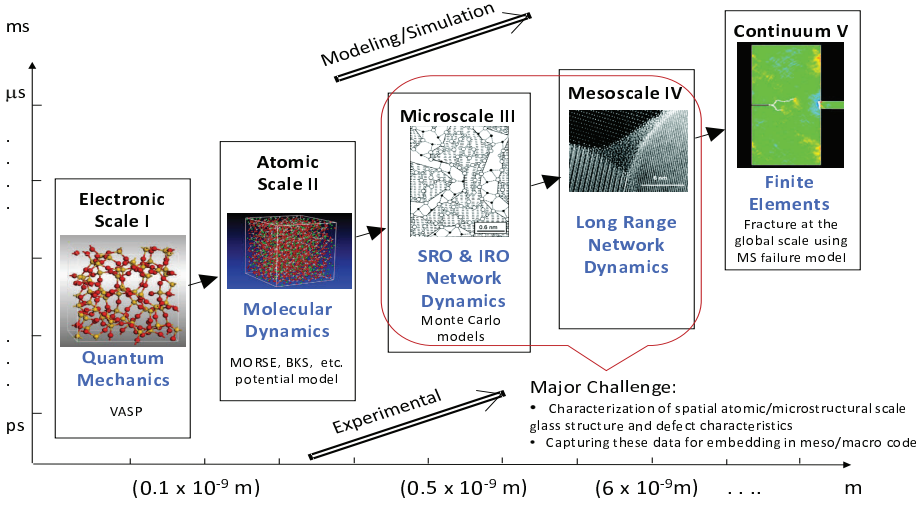

Figure 2. A multiscale model for non-crystalline ceramics (glass).

Specific long-term research goals are threefold:

1. Develop molecular dynamics (MD) process models for a series of chemically substituted amorphous silica (a-SiO_2 or fused silica) materials for the prediction of glass elastic properties assuming completely uniform glass "mesostructures." If successful, such models will enable ab initio prediction of structure-property relations in glass that will be validated with experimentally determined elastic properties.

2. Extend the MD models to study densification of chemically substituted a-SiO_2 materials under high pressures ($\sim$60 GPa Materials in Extreme Dynamic Environments [MEDE]) relevant to ballistic events where reversible and irreversible density changes and structural transformations have been observed. If successful, such models will enable ab initio prediction of a-SiO_2 compressibility, kinetics, and "glass" phase transformations that will be used to develop equations of state for a-SiO_2 materials, and thus form a direct link to the continuum scale.

3. Develop a fully validated multiscale finite element computational model and code incorporating the effects of reversible and irreversible densification, inelastic deformation, and overlain with a spatiotemporally evolving population of growing defects, which coalesce and lead to ultimate fracture and fragmentation. It is envisioned that at some time in the not too distant future, fully concurrent multiscale computational finite element codes will be used by analysts on a regular basis for optimal material design!

The remainder of the report is organized as follows. General program objectives are outlined in section 2, whereas the planned approach for modeling the multiscale behavior of glass is described in more detail in section 3. A one-day short course on "Glass Technology" held at the U.S. Army Research Laboratory (ARL) on October 29, 2010, is briefly described in section 4, followed by an overview of an ARL/Momentive Performance Materials purchase order for fabrication of pure and chemically substituted a-SiO_2 materials that will form the basis for future observational and computational efforts (section 5). First principle quantum mechanical methods are used to predict radial distribution functions (RDFs) in section 6; initial molecular dynamics models using simulated annealing are then used to develop a glass shock Hugoniot for fused silica in section 7. Initial efforts at computational modeling of plate impact experiments of fused silica appear in section 8. Section 9 summarizes the conclusions of the progress report.

2. Program Objectives

The long-term research goal of the program is to develop a concurrent multiscale computational finite element code for optimizing or enhancing the performance of various glasses against SCJs; the initial work focuses on pure fused-silica (a-SiO_2), and chemically varied a-SiO_2 materials. As such, this objective falls squarely within the purview of the Weapons and Materials Research Directorate (WMRD), since multiscale models are constitutive models (specific to a particular material) wherein time evolving microstructural changes, such as microcrack growth, are fully coupled to the macroscale, a phenomenon that cannot be modeled or accounted for using classical homogenization methods. A more immediate research objective is to understand why certain chemically substituted a-SiO_2 materials exhibit enhanced performance in the defeat of SCJ and other ballistic threats.

The program objectives are threefold:

1. Develop MD process models for a series of chemically substituted a-SiO_2 materials for the prediction of glass elastic properties. This glass plays an important role in many technological applications and its structure has been inferred from neutron-diffraction, nuclear magnetic resonance, and small angle x-ray scattering (SAXS) analysis to reveal a three-dimensional network consisting of tetrahedrally coordinated silicon (Si) whose structure is constant throughout the glass and defines its short range order (SRO). Long range disorder in the structure is manifested by a seemingly random variation in the Si-O-Si bond angle in adjacent tetrahedra. Despite the intense study of a-SiO_2 glass over the last several decades, much controversy still exists on the best method to model (i.e., via density functional theory, molecular dynamics, Monte Carlo methods, or master equation techniques) this archetypal material for prediction of elastic properties, diffusivity, surface interactions, bond angle distribution, polyamorphism, and melt solidification. Current models that appear in the literature are often not fully validated and progress towards this goal will be made when model predictions of elastic constants for a series of chemically substituted a-SiO_2 glasses agree with experimentally determined constants.

2. Extend the MD models to study densification of the chemically substituted a-SiO_2 materials under high pressures. Since long range order in glass is non-existent, variations in the SRO, and intermediate range order (IRO) must be responsible for the enhanced performance observed in ballistic tests on certain a-SiO_2 glasses. If this is the case,

it may be possible to use MD models to predict macroscopic ballistic performance. Since glass is subjected to extreme pressure and temperature during a SCJ event, it will be necessary to study the relationship between compressibility, kinetics, and phase transitions during high-pressure densification of a-SiO_2 glasses as manifested by changes in coordination number, ring size, and free volume. Progress towards this goal will be made when MD derived equations of state (EOS) agree with those obtained experimentally via diamond anvil press and plate impact experiments.

3. Develop a fully validated multiscale finite element computational model and code that incorporates the effects of reversible and irreversible densification, and inelastic deformation, overlain with a spatiotemporally evolving population of defects that grow, coalesce, and lead to ultimate fragmentation. This objective will develop a computational framework to combine the objectives from (1) and (2), and incorporate the influence of fracture initiation, growth, coalescence, and fragmentation of surface and volume defects in glass into a comprehensive concurrent multiscale finite element model and code. Microcrack initiation, growth, and coalescence (sometimes referred to as failure waves) is a multiscale phenomenon that bridges all scales in a-SiO_2 glasses despite the apparent absence of a structural mesoscale for this class of materials (see figure 2). Algorithms for the development of fully two-way coupled multiscale codes are in their infancy, and progress on this objective will be realized with successful development and implementation of a consistent scheme for coarse-graining localization phenomena such as fracture failure observed in glass.

3. Planned Approach

The planned approach consists of three components, which are outlined in figure 3:

1. Validate the MD models for a series of chemically substituted a-SiO_2 materials for the prediction of glass elastic properties. Although there is no effort within the WMRD to predict a-SiO_2 elastic properties, a hierarchical multiscale modeling effort is currently underway within WMRD, which is focused on the study of polycrystalline ($\sim$200 μm grain size) $AlON$ and validation of quantum and MD predictions of anisotropic elastic constants using diamond anvil cell and focused-ion-beam (FIB)/scanning electron microscopy (SEM) compression tests on oriented $AlON$ single crystals (*7*). We plan to use MD methods (with possible MD coarse-graining) to simulate glass process modeling during melt

solidification by quenching a high-density, high temperature, and pressure (with possible polyamorphic phases) melt for a series of chemically substituted a-SiO_2 materials. Next, the resulting room-temperature, chemically modified structures will be reversibly deformed to predict the elastic properties that will be validated with experimentally determined elastic properties.

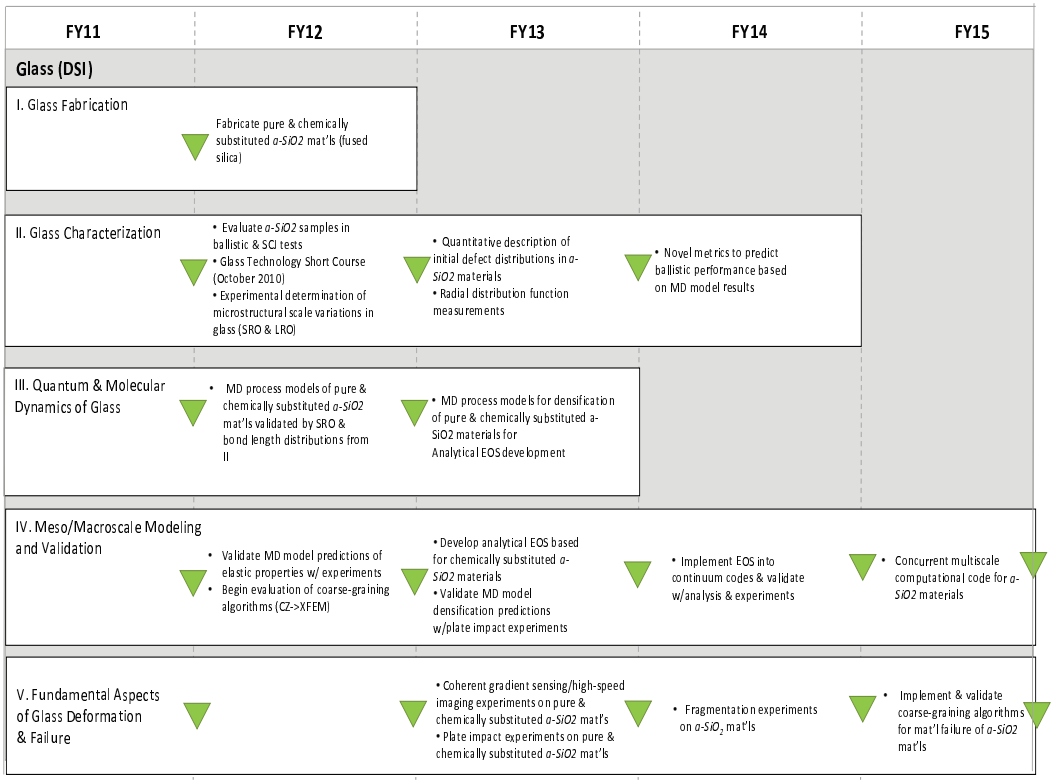

Figure 3. Five-year roadmap consistent with the WMRD brittle materials program.

2. Validate the MD models for densification of chemically substituted a-SiO_2 materials under high pressures. Although there is currently no effort within WMRD to predict the EOS of chemically substituted a-SiO_2 materials, MD methods have been used to predict high-pressure densification in these materials. MD simulations of pure a-SiO_2 materials reveal a Hugoniot elastic limit (HEL) of about 10 GPa, and an anomalous maximum in compressibility at around 3 GPa. Experiments where samples have been compressed to

pressures lower than 10 GPa are indistinguishable from the original material, whereas above 10 GPa, materials can sustain an irreversible density increase from 10–20% higher than the starting material, although there is controversy as to whether the mechanism is due to irreversible coordination defects or permanent ring size modification. In contrast to the behavior of a-SiO_2, crystalline quartz (α-SiO_2), undergoes very well-known high pressure polymorphic phase transitions into a Coesite phase and a Stishovite phase (figure 4), which involve changes in coordination of the Si cation from four to six O atoms. A combination of diamond anvil press and plate impact experiments will be conducted on a series of chemically substituted a-SiO_2 materials and compared with MD densification simulations in glass in order to understand the influence of glass modifiers on changes in the shock response of these materials. EOSs for a subset of promising chemically substituted materials will be developed and implemented into a continuum code to determine if any of the chemically substituted materials exhibit enhanced ballistic performance.

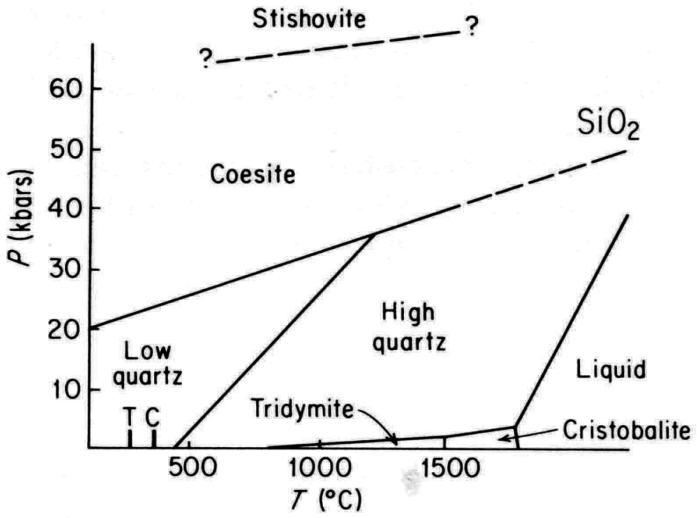

Figure 4. Crystal structures of quartz, after Frye (*2*).

3. Develop a fully validated multiscale finite element computational model and code that incorporates the effects of reversible and irreversible densification, and inelastic deformation, overlain with an spatiotemporally varying population of defects which grow, coalesce, and lead to ultimate material fragmentation. The ultimate research objective is to develop a physics-based multiscale computational finite element code for studying densification, and

dynamic fracture in non-crystalline ceramics (see figure 2). Atomistic behavior will be linked to macroscopic elastic properties and densification behavior through development of an EOS from first principles as outlined in (1) and (2) above. At this stage, what remains to be accomplished, is to successfully link, in a concurrent fashion, multiscale failure phenomena in a-SiO_2 materials by incorporating the important role that pre-existing surface and volume defects have on the microcrack growth, coalescence, and fragmentation in this class of materials. Over the past five years, the first author has also been directly involved in development of a parallel, concurrent multiscale code for heterogeneous viscoelastic composites (*8*) under the auspices of an ARL/University of Nebraska cooperative agreement, which will be leveraged and used as the framework for the development of a concurrent multiscale model of a-SiO_2 materials. The chief challenge for brittle materials is to correctly account for the growth kinetics of microcracks in a multiscale computational environment. The propagation of free internal boundaries at lower scales will be "coarse-grained," to higher scales where global fracture failure and fragmentation is observed. As such, coarse-graining algorithms will need to be validated through continuum-scale experiments on a-SiO_2 materials that measure dynamic crack propagation speeds, mixed-mode failure, and crack bifurcation phenomena using coherent gradient sensing and high speed imaging techniques; ARL possesses capabilities for conducting such dynamic fracture experiments in a-SiO_2 materials through the recent establishment of a coherent gradient sensing/imaging facility funded by the ongoing multiscale modeling effort of $AlON$. Models and validation of the initiation and propagation of discrete fractures in a-SiO_2 materials should transition naturally into models of fragmentation and comminution for behind-armor-debris applications. Fragmentation experiments have classically been conducted using dynamically expanding ring experiments for defining fragment size versus strain rate and will be used to validate computational models of fragmentation. The development of consistent coarse-graining algorithms for fracture in materials, which is associated with failure and loss of material stability, is largely unexplored and is the primary high-risk goal of this section.

4. Glass Technology Short Course

A one-day short course on the "Fundamentals of Glass Science," was taught by Professor Arun K. Varshneya, Alfred University, at ARL on October 29, 2010. Course attendees received copies of Varshneya's *Fundamentals of Inorganic Glasses* (*3*). The course covered topics on (1) basic compositions and families of commercial glasses that include vitreous silicates, soda-lime silicates, borosilicates, lead silicates, and aluminosilicates; (2) fundamentals of the glassy state; (3) phase separation and liquid-liquid immiscibility; (4) glass structures: oxide and non-oxide glasses; (5) review of some glass properties (e.g., elastic properties, hardness, viscosity, thermal expansion, durability); and (6) annealing and strengthening.

The course was well received, and a question and answer period ensued with questions like, "What is the difference between a glass and an amorphous material?" Answer: "Amorphous materials make a continuous or discontinuous volume transition to a crystal or vapor on heating, whereas, glasses continuously change to a liquid on heating." See also, p. 17 and 18 in Varshneya (*3*), and figure 5.

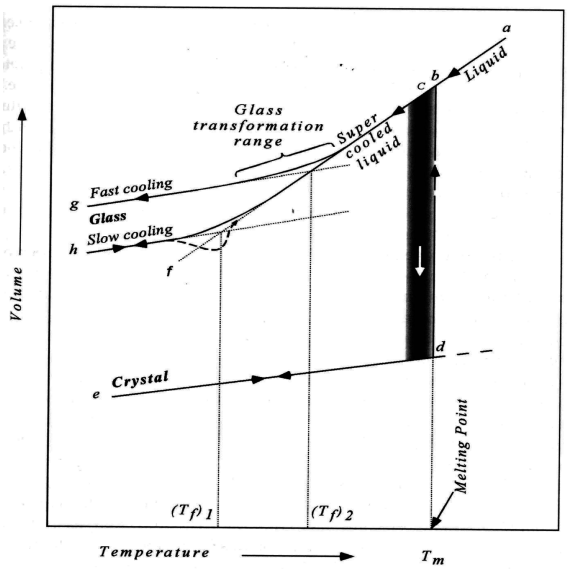

Figure 5. The volume-temperature diagram for a glass-forming liquid, after Varshneya (*3*).

5. ARL/Momentive Performance Materials, Inc. White Paper Proposal

The following sections are quoted from the Momentive Performance Materials, Inc.* white paper proposal.

5.1 Goal:

The goal of the work outlined in this proposal is to produce several unique high silica glasses and submit them to the Army Research Laboratory for ballistic performance evaluation. Utilizing our internal capabilities and those of our partners we will propose select glass compositions and evaluate the glasses in terms of thermomechanical, chemical, and mechanical properties. A select subset of glasses will then be produced in a form suitable for ballistic testing. While this brief study will not allow us to elucidate all the complex interactions between of glass composition and ballistic mechanical properties, this scoping trial should give us some guidance as to how much additional improvement might be possible in high-silica, low density glasses with additional research.

5.2 Background:

While there are inevitable tradeoffs between weight and ballistic performance, improvements to the base material can offer significant benefits to a previously optimized package. For instance, fused silica has a better stopping power and a lower density than soda-lime-silica glass resulting in a higher performance/mass figure of merit . However, fused silica suffers from a large amount of secondary fracture created during the initial impact making the window less clear and probably reducing it's resistance to further impacts. While the cause of this is not understood, one might surmise that it is driven by the atomic structure of the glass (i.e. number of non-bridging O, ring density, etc.) that can be impacted by the chemistry of the glass. These compositional and structural differences affect how the impact energy transfers within the glass and where the energy absorbing fractures take place. For example, Sehgal and Ito (*4*) found that changes in density of silica glass had a large impact on brittleness (see figure 6 below from Sehgal and Ito (*4*)). If a reduction in brittleness translates to improved (reduced) secondary fracture and it can be

*Richmond Heights, OH 44143

accomplished without substantially increasing the density of the glass (i.e. staying near high-silica glass compositions) then significant optimization might be possible.

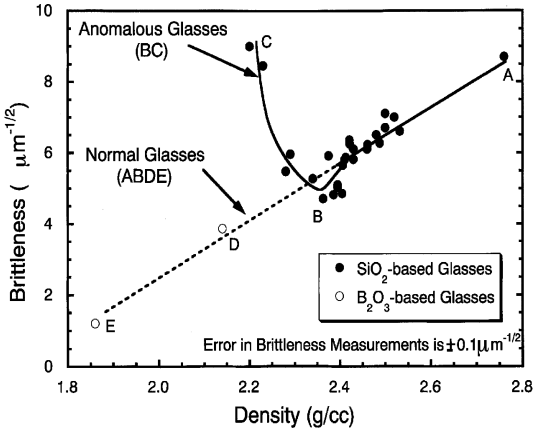

Figure 6. Brittleness versus density for glasses in the SiO_2 and B_2O_3-based glasses, after Sehgal and Ito (*4*).

5.3 Approach:

We will produce high silica glasses with additions of up to 10 wt% of network formers and modifiers using Momentive's lab scale puck fusion process at temperatures up to 1900C. These glasses will be characterized (density, UV-Vis transmission) and evaluated mechanically to determine their hardness and "brittleness" following the methods outlined in references (*4, 9*), In addition, viscosity data will be collected to assist in selecting proper temperatures for larger scale melting of the glasses in phase 2. Candidate compositions from phase one that might exhibit improved secondary fracture will be melted in phase 2 using our 200 lb ingot test melter. These ingot samples will be large enough to produce several 12"x12" windows. The cut and polished windows will be furnished to ARL for assembly and ballistic testing to validate the small scale mechanical testing results and determine whether these relatively minor changes in composition can significantly affect the secondary cracking phenomenon and result in an optimized high silica glass.

To date, fused silica samples have been delivered to ARL and have been ballistically tested.

6. Quantum Mechanics Modeling of Glass

We used a first principles quantum mechanics method, the Vienna ab initio simulation package (VASP) (*10*) to optimize the amorphous structure of a continuous random network, generated by a Monte Carlo bond switching model (*11*). A projector augmented-wave basis with an energy cutoff of 600 eV was used. Brillouin-zone integrations were carried out using two special k points. Atomic relaxations were performed until the maximum forces on atoms became less than 0.01 eV/Å; reaction barriers were calculated using the elastic-band method. Convergence tests indicate that the energies reported have an uncertainty of less than 0.05 eV.

The optimized structures have different densities (2.04–2.25 g/cm^3), different numbers of atoms (72, 114, and 192), and different distributions of atoms in the rings (3–7 member rings in the structure shown in figure 7(a) and 4–6 rings in the structures shown in figures 8(a) and 9(a)) of random continuous networks. The model has an amorphous structure inside the unit cell and periodic boundary conditions, and was found quite efficient for probing of the interaction of hydrogen containing fractions with network of silica (*12*). RDFs (atomic density variations with distance from a particular atom) calculated for these structures are presented in figures 7(b), 8(b), and 9(b). Positions of two first peaks are in reasonable agreement with experimental RDF obtained from x-ray diffraction (*13*). The calculation of bulk modulus, B, from a strain-energy relationship and simple hydrostatic pressure for a cubic unit cell with 114 atoms depicted in 8(a) resulted in B = 40.6 GPa. We plan to calculate the bulk modulus and elastic constants for other optimized models of silica.

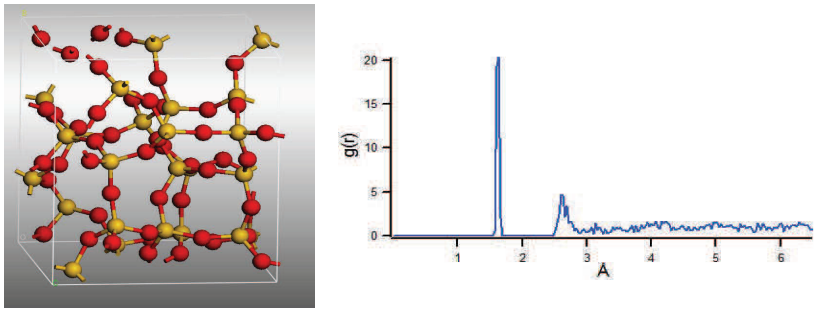

(a) (b)

Figure 7. (a) 72-atom unit cell with density 2.15 g/cm^3 and (b) corresponding RDF.

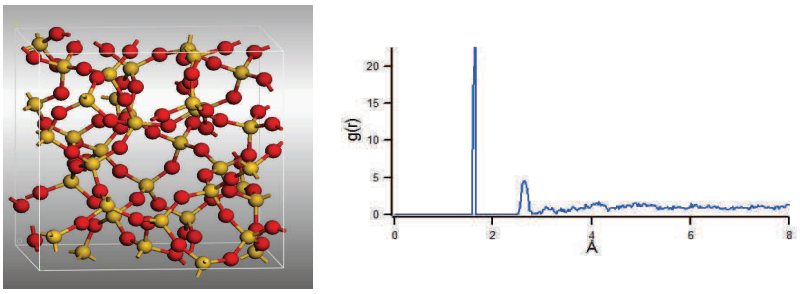

(a) (b)

Figure 8. (a) 114-atom unit cell with density 2.25 g/cm^3 and (b) corresponding RDF.

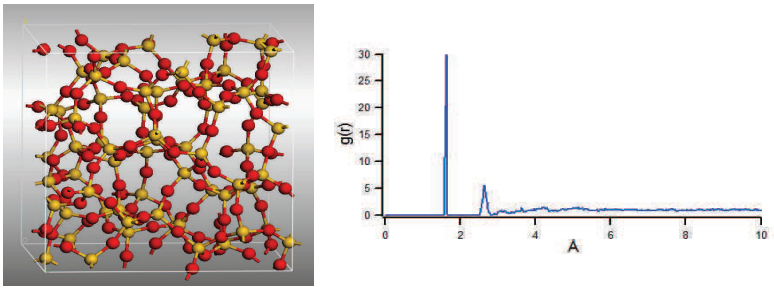

(a) (b)

Figure 9. (a) 192-atom unit cell with density 2.18 g/cm^3 and (b) corresponding RDF.

7. Molecular Dynamics Modeling of Glass

Time-dependent processes for large condensed phase systems are modeled at the atomic scale using MD, in which classical equations of motion for a system of atoms are integrated in time (a "trajectory"). Thermodynamic properties can also be determined for systems at equilibrium, through which time averages are obtained from states sampled over the duration of the trajectory. This method will be used to study the response of glasses that have been subjected to shock loading or to and characterize properties that might assist in understanding failure of these materials. The MD method we are using is limited by the classical approximation and an accurate description of the interatomic interactions for the system, denoted hereafter as the potential energy surface (PES). It is particularly important that the PES properly describe the system under study before it can be used in a predictive capacity. Fortunately, there are numerous atomistic models for silicate glasses that have been developed for various MD simulation studies. For this year's effort, we used MD predictions of the shock Hugoniot of amorphous silica for verification and validation of the various models, with a goal to identify reasonable models for use in future MD explorations of material properties at high loading rates.

7.1 Interatomic Potentials

Although numerous MD models of silica and modified silicate glasses exist, we have focused on two interatomic potentials for silica. These were selected for initial exploration because of their extensive validation over a wide range of thermodynamic states and because they had parameters for the chemically substituted systems of interest (i.e., calcium [Ca], sodium [Na], and aluminum [Al]). The first potential has the following form

$$U(r) = \frac{kq_iq_j}{r^2} + D_{ij}\left[\{1 - \exp\left(-a_{ij}\cdot(r - r_0)\right)\}^2 - 1\right] + \frac{C_{ij}}{r^{12}} \quad , \tag{1}$$

where k, q_i, q_j, D_{ij}, a_{ij}, r_0, and C_{ij} are constants, which are provided in Pedone et al. (*14*). The first term is a long-range Coulomb interaction, which is accurately evaluated through the Ewald summation (*15*) in MD simulations assuming a finite simulation cell with periodic boundary conditions imposed, the second term is a short-range Morse function, and the last is a purely repulsive term. For simplicity, we will refer to equation 1 as a Morse potential. A second potential was also used in this study, a Buckingham potential in the form

$$U(r) = \frac{kq_iq_j}{r^2} + A_{ij}\exp\left(-\frac{r_{ij}}{\rho}\right) + \frac{C_{ij}}{r^6} \quad , \tag{2}$$

where k, q_i, q_j, A_{ij}, r_{ij}, ρ, and C_{ij} are constants, which are provided by van Beest et al. (*16*); we refer to equation 2 as the BKS potential.

7.2 Generating Equilibrated Initial Structure of Fused Silica

We started with 1536 molecules (1536 Si atoms and 3072 O atoms) of quartz crystal in the β-cristobalite phase. This is a tetragonal phase; in order to generate a cubic simulation cell, the z-dimension was reduced to equal the x- and y-dimensions, and the dimensions of the simulation cell are chosen so that the density of the material is equal to the experimental value of 2.20 g/cm^3. This compression introduces considerable stress to the system; however, this is not a concern as very high stresses are obtained during the annealing process.

To generate an amorphous phase, we anneal a system from a melt by decreasing the temperature in discrete intervals. The system is simulated in the constant volume-constant temperature (NVT) ensemble to ensure the density remains constant. We used the molecular dynamics code LAMMPS (*17*), which is equipped to support this annealing method within a single simulation run.

Using the Morse potential (equation 1), the temperature was decreased in discrete intervals following the schedule provided in Pedone et al. (*14*). Starting at 5000 K, the system was equilibrated by scaling the velocity every time step for 6000 steps, then scaling was reduced to every 40 time steps for 6000 steps, and finally velocity scaling was turned off for the final 8000 steps. The temperature of the system was then decreased by 500 K, and the process was repeated until the temperature of the system reached 300 K. This results in a total simulation time of 470 ps, which is a nominal cooling rate of 10 K/ps.

7.3 Characterizing Fused Silica

The final configuration from the annealing simulation described in the previous section was used as the initial configuration in constant pressure-constant temperature (NPT) simulations using both forms of the interatomic potential (equations 1 and 2). All simulations in this section were run using the DL_POLY MD suite of codes (*18*). The timestep for the NPT simulations was 0.2 fs, with barostatting and thermostatting rates of 0.5 and 1.0 ps, respectively. The simulations were run for 60 ps, following a 10-ps equilibration with velocity scaling every 10 time steps. The results were analyzed to obtain structural details of the amorphous material.

Our first criterion in evaluating the interatomic potential is the ambient state density, which we compare to the experimental value of 2.20 g/cm^3. The Morse potential resulted in a density of 2.26 g/cm^3, slightly higher than the experimental value, while the BKS potential produced an even higher density of 2.34 g/cm^3. The density of the Morse potential is within 3% of the experimental value, but the error in the BKS density is greater than 6% , which is higher than typically acceptable. We also calculated partial RDFs for the three atomic pairs, Si-O, Si-Si and O-O, using both potentials. The difference in RDFs between the Morse and BKS potentials was negligible; hence, in figure 10 we compare the Morse potential RDFs to those from a shell model potential for silica (*5*). Except for a slight difference in the height of the first peak, figures 10(a) and 10(b) are nearly identical. This indicates that the Morse and BKS models accurately capture the expected structure of fused silica. We note that the Tilocca et al. (*5*) model was not considered for use in this project due to numerical difficulties associated with integrating trajectories using this model under compression.

Finally, we calculate the Hugoniot curve for the two potentials, following the method of Erpenbeck (*19*). The Hugoniot function is

$$H(T,V) = E(T,V) - E_0(T_0,V_0) + \tfrac{1}{2}\left[P(T,V) + P_0(T,V)\right](V - V_0) \quad , \tag{3}$$

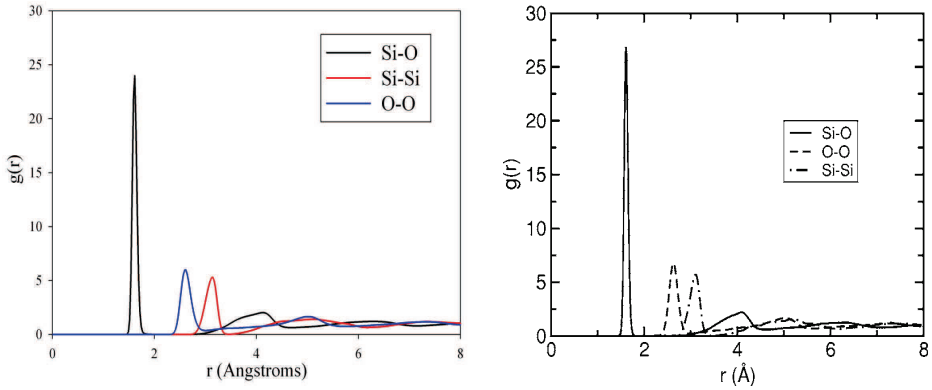

(a) (b)

Figure 10. RDFs of (a) our system using the Morse potential and (b) system in Tilocca et al. (*5*).

where T and P represent the temperature and pressure, V and E represent the volume/unit mass and internal energy/unit mass, and the subscript 0 indicates the unshocked reference state. A Hugoniot curve represents a set of (P, V, T) points for which equation 3 is equal to zero. To calculate a single point, a series of constant volume-constant temperature (NVT) simulations is performed over a range of temperatures, all at the same volume. The Hugoniot as a function of temperature is fitted to a polynomial, and the $H = 0$ value is interpolated. (For our calculations, a linear fit was sufficient to extract the Hugoniot temperature). Pressure data as a function of temperature can then be fitted to a polynomial to determine the corresponding pressure at the Hugoniot temperature. Figure 11 shows the Hugoniot curves for both the Morse and BKS potentials, represented as pressure versus volume ratio (V/V_0 or relative volume), as well as the experimental values for comparison. We see that at high values of V/V_0, the Morse potential is nearly in agreement with experimental results, while at low values of V/V_0 the pressure is too high. Conversely, the BKS potential shows better agreement at low values of V/V_0, but the pressure is too low at higher values of V/V_0. We performed several numerical experiments in which we scaled various parameters of the two PES functions in order to obtain good agreement of the shock Hugoniot at both high and low densities; however, any improvement in the Hugoniot curve corresponded to an increased error in the density. The discrepancies between our Hugoniot curves and the experimental values render these models inadequate for our modeling requirements. We are continuing to evaluate other a-SiO_2 atomistic models, as well as exploring the possibility of fitting parameters using force matching techniques of Izvekov et al. (*20*).

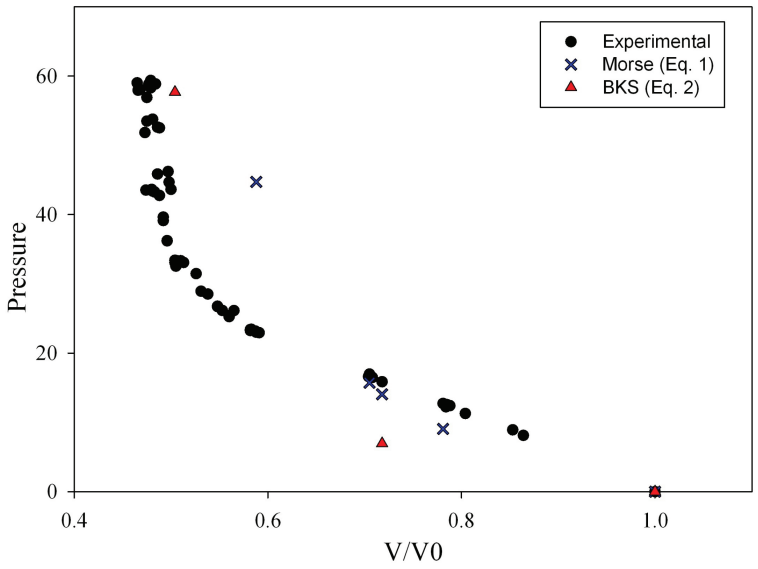

Figure 11. Comparison of Hugoniot curve of fused silica (a-SiO_2): experiment (●), Morse potential (×) and BKS potential (▲).

8. Equation-of-state Modeling of Glass

Validation of the equation of state (EOS) constructed from multiscale modeling will be through comparison with continuum data. Bulk modulus data exist in the literature for several common SiO_2-based glasses measured in high pressure fixtures and diamond anvil cells (DACs) for pressures up to approximately 10 GPa. Similar quasi-static data can be extracted for the compositions examined in this study if resources permit. In the neighborhood of approximately 10 GPa pressure, many glasses begin permanent rearrangement on the atomic scale. While it is possible to continue measurement of bulk modulus in a DAC beyond this point, there is no established way to measure density in the amorphous glasses. Consequently, validating the model predictions at higher pressure with quasi-static data will be challenging. Experimental techniques development is needed to pursue validation at higher quasi-static pressures. Alternatively, EOS model validation at high pressures can also be accomplished through comparison with Hugoniot data from shock experiments. One must also be careful when using the shock data, but the approximations in the data interpretation tend to diminish as pressure increases. Two of the features that must be dealt with are strength and non-recoverable volume

change. To determine the extent to which these features complicate the data, finite element simulations replicating symmetric impact, gas gun Hugoniot experiments were run in ALE3D (*21*) using the Livermore Equation of State (LEOS) tables for fused silica. The simulations were run with and without strength to quantify the differences. The constant strength model is used to introduce a limit to the elastic shear response. Data on inelastic shear strength as a function of deformation were not found in the literature, so the constant flow strength is a crude approximation for a behavior that likely depends on density, strain, strain rate, pressure, and temperature. Figure 12 presents the axial stress distribution at the shock front for an impact velocity of 4 km/s. Shown is the expected three-wave structure (traveling to the right in the plot), with the first step due to the limit on the elastic shear stiffness and the second due to the volume collapse.

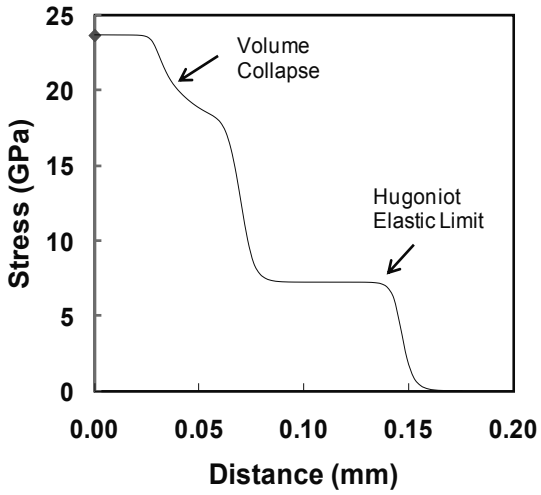

Figure 12. Stress wave distribution in fused silica.

The wave front is not steady at this lower impact pressure in that the three-wave fronts continue to separate over time. A steady wave is assumed when analyzing data in the context of the Hugoniot equations, and that introduces uncertainty when computing the energy dissipation and stress. One is faced with the question of which wave front to use to compute the wave speed when analyzing the data. The experimental results under these low pressure conditions must be put in the context of how the data were reduced. At higher impact pressures, the plastic wave and the transformation front both overtake the elastic precursor and create a strong shock. Under these higher pressure conditions, the data analysis is not ambiguous.

The plot in figure 13 provides some indication of the error in the energy calculation. The error metric plotted is the difference between the energy computed by the finite element code and the ideal energy computed assuming the Hugoniot relations apply. Normalization is by the ideal energy. It can be seen that the deviation from the Hugoniot conditions is significant at lower compressions but nearly zero at densities above 4.3 g/cm^3. This coincides with development of a strong shock as described previously. It should also be noted that the energy error is significantly greater for the calculation with strength. The energy from inelastic dissipation is not captured properly by the Hugoniot energy balance in the low pressure regime where the elastic precursor outpaces the plastic wave. The error vanishes when the plastic wave overtakes the elastic precursor and the wave becomes steady.

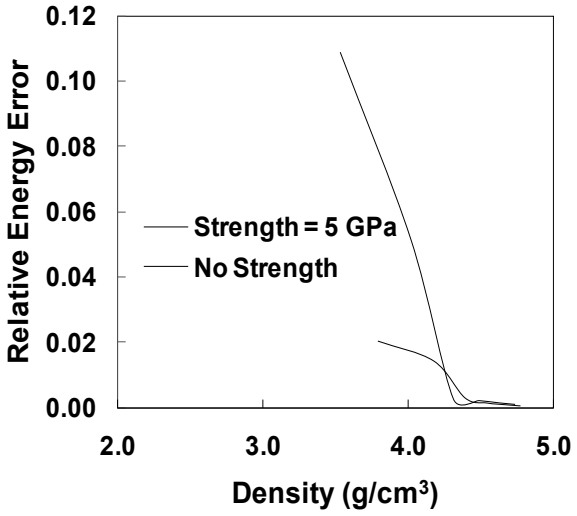

Figure 13. Energy error vs. density in fused silica.

The stress density plots from the simulations are shown along with data by Marsh (*6*) in figure 14. It can be seen that the LEOS table reproduces the data reasonably well in the high pressure range. The strength used in the simulations can make an appreciable difference at lower pressure but because the strength was specified as constant rather than pressure dependent, the relative influence decays as the pressure increases. Simulations were not run at lower pressures because the results are increasingly dominated by the assumed strength model and volume collapse, neither of which is thought to be accurate in these simulations. The initial density is 2.204 g/cm^3, so there is a significant span of density change where the volume collapse and strength dominate.

These simple analyses illustrate that strength effects on gas gun results for glass can be appreciable, because the strength is a significant fraction of the total stress. The strength and whether or not the waves are steady should be considered when using the data to calibrate an EOS or validate multiscale results.

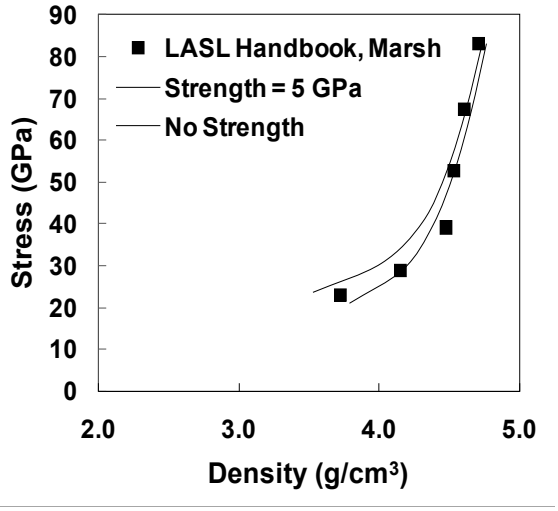

Figure 14. Stress wave vs. density in fused silica compared with data from Marsh (*6*).

9. Conclusions

This six-month progress report on multiscale modeling of noncrystalline ceramics (glass) has focused on establishing the framework for development of a multiscale computational methodology for optimizing or enhancing the performance of fused silica materials not yet synthesized. A more immediate research objective is to understand why certain chemically substituted fused silica materials exhibit enhanced performance in the defeat of SCJs and other ballistic threats. Conclusions consistent with the milestones shown in the five-year roadmap shown in figure 3 are as follows:

1. Professor Arun K. Varshneya of Alfred University, gave a short course on "Fundamentals of Glass Science," at the ARL on October 29, 2010; course attendees received copies of *Fundamentals of Inorganic Glasses* (*3*), as well as a variety of practical considerations regarding glass formation and technology.

2. Fused silica specimens have been delivered to ARL under the auspices of an ongoing cooperative agreement; these specimens have been ballistically tested, and will serve to validate future computational models of fused silica.

3. A first principles quantum mechanics method (VASP) (*10*) was used to optimize the amorphous structure of a continuous random network, generated by a Monte Carlo bond switching model (*11*). A projector augmented-wave basis with an energy cutoff of 600 eV was used. The optimized structures have different densities (2.04–2.25 g/cm^3), different numbers of atoms (72, 114, and 192), and different distributions of atoms in the rings (3–7 member rings in the structure shown in figure 7(a) and 4–6 rings in the structures shown in figures 8(a) and 9(a)) of random continuous networks. RDFs calculated for these structures are presented in figures 7(b), 8(b), and 9(b). Positions of two first peaks are in reasonable agreement with experimental RDF obtained from x-ray diffraction (*13*).

4. Initial fused silica glass structures were generated via LAMMPS (*17*) simulations by simulated annealing the system from a melt via a Morse potential (equation 1) using the schedule provided in Pedone et al. (*14*). Final configurations from the simulated annealing runs were used as the initial configurations for DL_POLY (*18*) predictions of RDFs for fused silica, which compared favorably with the results of Tilocca et al. (*5*);

5. Hugoniot curves for fused silica were calculated using the method of Erpenbeck (*19*) using both Morse and BKS potentials. The Morse potential accurately models pressure at a relative volume greater than 0.7, yet overpredicts pressure at a lower relative volume. The BKS potential accurately predicts pressure at a relative volume on the order of 0.5, but underpredicts pressure at larger relative volumes. The discrepancies between the computed Hugoniot values and experimental data render these potentials inadequate for our modeling requirements, and we are evaluating other a-SiO_2 atomistic models, as well as exploring the possibility of fitting parameters using force matching techniques of Izvekov et al. (*20*).

6. Symmetric gas gun impact simulations on fused silica were conducted using the ALE3D code based on data from the LEOS tables. The classic three-wave structure was observed in the fused silica simulations, and stress versus density calculations reproduced the experimental data reasonably well in the high pressure range. The strength used in the simulations can make an appreciable difference at lower pressure because the strength was specified as constant rather than pressure dependent, and it was shown that the relative influence decays as the pressure is increased.

10. References

1. Moran, B.; Glenn, L. A.; Kusubov, A. Jet Penetration in Glass. *J. Phys. IV* **1991**, *1 (C3)*, 147–154.

2. Frye, K. *Modern Mineralogy;* Prentice-Hall, Inc.: Englewood Cliffs, NJ, 1974.

3. Varshneya, A. K. *Fundamentals of Inorganic Glasses;* 2^{nd} ed.; Society of Glass Technology: Sheffield, 2006.

4. Sehgal, J.; Ito, S. Brittleness of Glass. *J. Non-Cryst. Solids* **1999**, *253*, 126–132.

5. Tilocca, A.; de Leeuw, N. H.; Cormack, A. N. Shell-model Molecular Dynamics Calculations of Modified Silicate Glasses. *Phys. Rev. B* **2006**, *73* (10), 104209.

6. Marsh, S. P., Ed. *LASL Shock Hugoniot Data;* University of California Press: Berkeley, CA, 1980.

7. Gazonas, G. A.; McCauley, J. W.; Batyrev, I. G.; Casem, D.; Clayton, J. D.; Dandekar, D. P.; Kraft, R.; Love, B. M.; Rice, B. M.; Schuster, B. E.; Weingarten, N. S. Multiscale Modeling of Armor Ceramics: Focus on AlON. *Proceedings of the 27^{th} Army Science Conference* **2010**, *to appear.*

8. Souza, F. V.; Allen, D. H. Multiscale Modeling of Impact on Heterogeneous Viscoelastic Solids Containing Evolving Microcracks. *Int. J. Numer. Meth. Eng.* **2010**, *82* (4), 464–504.

9. Ito, S. Structural Study on Mechanical Behavior of Glass. *J. Ceram. Soc. Jpn.* **2004**, *112* (1309), 477–485.

10. Kresse, G.; Hafner, J. Norm-conserving and Ultrasoft Pseudopotentials for First-row and Transition-elements. *J. Phys.: Condens. Mat.* **1994**, *6* (40), 8245–8257.

11. Tu, Y. H.; Tersoff, J.; Grinstein, G.; Vanderbilt, D. Properties of a Continuous-random-network Model for Amorphous Systems. *Phys. Rev. Lett.* **1998**, *81* (22), 4899–4902.

12. Batyrev, I. G.; Tuttle, B.; Fleetwood, D. M.; Schrimpf, R. D.; Tsetseris, L.; Pantelides, S. T. Reactions of Water Molecules in Silica-based Network Glasses. *Phys. Rev. Lett.* **2008**, *100* (10), 105503.

13. Konnert, J. H.; D'Antonio, P.; Karle, J. Comparison of Radial-Distribution Function for Silica Glass with Those for Various Bonding Topologies - Use of Correlation-function. *J. Non-Cryst. Solids* **1982**, *53* (1-2), 135–141.

14. Pedone, A.; Malavasi, G.; Menziani, M. C.; Cormack, A. N.; Segre, U. A New Self-consistent Empirical Interatomic Potential Model for Oxides, Silicates, and Silica-based Glasses. *J. Phys. Chem. B* **2006**, *110* (24), 11780–11795.

15. Ewald, P. P. Die Berechnung Optischer und Elektrostatischer Gitterpotentiale. *Ann. Phys.* **1921**, *369*, 253–287.

16. van Beest, B. W. H.; Kramer, G. J.; van Santen, R. A. Force-fields for Silicas and Aluminophosphates Based on Ab Initio Calculations. *Phys. Rev. Lett.* **1990**, *64* (16), 1955–1958.

17. Plimpton, S. J. *LAMMPS Users Manual: Large-scale Atomic/Molecular Massively Parallel Simulator;* Sandia Corporation: Sandia National Laboratories, 2003.

18. Todorov, I. T.; Smith, W. *The DL_POLY 4 User Manual, Version 4.01.0;* STFC Daresbury Laboratory: Daresbury, Warrington WA4 4AD, Cheshire, UK, 2010.

19. Erpenbeck, J. J. Molecular-dynamics of Detonation. 1. Equation of State and Hugoniot Curve for a Simple Reactive Fluid. *Phys. Rev. A* **1992**, *46* (10), 6406–6416.

20. Izvekov, S.; Parrinello, M.; Burnham, C. J.; Voth, G. A. Effective Force Fields for Condensed Phase Systems From ab initio Molecular Dynamics Simulation: A New Method for Force-matching. *J. Chem. Phys.* **2004**, *120* (23), 10896–10913.

21. Nichols, A. *Users Manual for ALE3D: An Arbitrary Lagrange/Eulerian 2D and 3D Code System;* Lawrence Livermore National Laboratory, LLNL-SM-433954: Livermore, CA, 2010.

List of Symbols, Abbreviations, and Acronyms

α-SiO_2	crystalline quartz
Al	aluminum
ALE3D	arbitrary Lagrangian-Eulerian three dimensional hydrocode
$AlON$	aluminum oxynitride
ARL	U.S. Army Research Laboratory
a-SiO_2	fused silica or amorphous quartz
BKS	MD potential named after authors (*16*)
Ca	calcium
DAC	diamond anvil cell
DL_POLY	MD code named after developers at Daresbury Laboratory
DSI	Director's Strategic Inititiative
EOS	equation of state
FIB	focused-ion-beam
HEL	Hugoniot elastic limit
IRO	intermediate range order
LAMMPS	large-scale atomic/molecular massively parallel simulator
LEOS	Livermore equation of state
MD	molecular dynamics
Na	sodium
MEDE	materials in extreme dynamic environments
NPT	constant pressure-constant temperature
NVT	constant volume-constant temperature
O	oxygen
PES	potential energy surface
RDF	radial distribution function
SAXS	small angle x-ray scattering
SCJ	shaped charge jet
SEM	scanning electron microscopy
Si	silicon
SiC	silicon carbide
SRO	short range order
VASP	Vienna ab initio simulation package
WMRD	Weapons and Materials Research Directorate

INTENTIONALLY LEFT BLANK.

NO. OF COPIES	ORGANIZATION
1 (PDF ONLY)	DEFENSE TECHNICAL INFORMATION CTR DTIC OCA 8725 JOHN J KINGMAN RD STE 0944 FORT BELVOIR VA 22060-6218
1	DIRECTOR US ARMY RESEARCH LAB IMNE ALC HRR 2800 POWDER MILL RD ADELPHI MD 20783-1197
1	DIRECTOR US ARMY RESEARCH LAB RDRL CIM L 2800 POWDER MILL RD ADELPHI MD 20783-1197
1	DIRECTOR US ARMY RESEARCH LAB RDRL CIM P 2800 POWDER MILL RD ADELPHI MD 20783-1197
1	DIRECTOR US ARMY RESEARCH LAB RDRL D 2800 POWDER MILL RD ADELPHI MD 20783-1197
	ABERDEEN PROVING GROUND
1	DIR USARL RDRL CIM G (BLDG 4600)

NO. OF COPIES	ORGANIZATION
2	NSF S MCKNIGHT G PAULINO 4201 WILSON BLVD, STE 545 ARLINGTON, VA, 22230-0002
3	DARPA L CHRISTODOULOU W COBLENZ J GOLDWASSER 3701 N FAIRFAX DR ARLINGTON VA 22203-1714
1	DIRECTOR US ARMY ARDEC AMSRD AAR AEE W E BAKER BLDG 3022 PICATINNY ARSENAL NJ 07806-5000
1	COMMANDER US ARMY RSRCH OFC RDRL ROE N B LAMATTINA PO BOX 12211 RESEARCH TRIANGLE PARK NC 27709-2211
1	COMMANDER US ARMY RSRCH OFC RDRL ROE M D STEPP PO BOX 12211 RESEARCH TRIANGLE PARK NC 27709-2211
1	RUTGERS UNIVERSITY DEPT MATLS SCI & ENGRG R LEHMAN 607 TAYLOR ROAD PISCATAWAY, NJ 08854
1	CLEMSON UNIV DEPT OF MECH ENGRG M GRUJICIC 241 ENGRG INNOVATION BLDG CLEMSON SC 29634-0921
1	UNIVERSITY OF MISSISSIPPI DEPT OF MECH ENGRG A M RAJENDRAN 201-B CARRIER HALL UNIVERSITY, MS 38677
2	SRI INTERNATIONAL D CURRAN D SHOCKEY 333 RAVENSWOOD AVE MENLO PARK CA 94025
1	INST OF ADVANCED TECH UNIV OF TX AUSTIN S BLESS 3925 W BRAKER LN STE 400 AUSTIN TX 78759-5316
5	SOUTHWEST RSRCH INST C ANDERSON K DANNEMANN T HOLMQUIST G JOHNSON J WALKER PO DRAWER 28510 SAN ANTONIO TX 78284
1	APPLIED RSCH ASSOCIATES D E GRADY 4300 SAN MATEO BLVD NE STE A220 ALBUQUERQUE NM 87110
2	WASHINGTON ST UNIV INST OF SHOCK PHYSICS Y M GUPTA J ASAY PULLMAN WA 99164-2814
1	JOHNS HOPKINS UNIV DEPT OF MECH ENGRG K T RAMESH LATROBE 122 BALTIMORE MD 21218
1	UNIV OF TEXAS-PAN AMERICAN COLLEGE OF ENGRG & COMPUTER SCI D H ALLEN 1201 WEST UNIVERSITY DR EDINBURG, TX 78539-2999
1	UNIV OF DAYTON RSRCH INST N S BRAR 300 COLLEGE PARK MS SPC 1911 DAYTON OH 45469

NO. OF COPIES	ORGANIZATION
4	RDRL D C CHABALOWSKI J CHANG R SKAGGS V WEISS BLDG 205 2800 POWDER MILL RD ADELPHI MD 20783-1197
	ABERDEEN PROVING GROUND
79	DIR USARL RDRL WM B FORCH S KARNA J MCCAULEY P PLOSTINS P BAKER RDRL WML D LYONS J NEWILL M ZOLTOSKI RDRL WML B I BATYREV B RICE N WEINGARTEN RDRL WML D P CONROY M NUSCA RDRL WML G M BERMAN W DRYSDALE RDRL WML H D SCHEFFLER S SCHRAML B SCHUSTER RDRL WMM J BEATTY R DOWDING RDRL WMM A M MAHER J TZENG E WETZEL RDRL WMM B T BOGETTI B CHEESEMAN C FOUNTZOULAS A GAZONAS G GAZONAS D HOPKINS P MOY

NO. OF COPIES	ORGANIZATION
	B POWERS C RANDOW T SANO M VANLANDINGHAM R WILDMAN C F YEN RDRL WMM C J LA SCALA RDRL WMM D E CHIN K CHO RDRL WMM E J ADAMS M COLE T JESSEN J LASALVIA P PATEL J SANDS RDRL WMM F L KECSKES H MAUPIN RDRL WML G J ANDZELM A RAWLETT RDRL WMP S SCHOENFELD RDRL WMP B R BECKER S BILYK D CASEM J CLAYTON M GREENFIELD C HOPPEL R KRAFT B LEAVY B LOVE M RAFTENBERG S SATAPATHY M SCHEIDLER T WEERASOOYIA RDRL WMP C T BJERKE S SEGLETES RDRL WMP D R DONEY D KLEPONIS J RUNYEON B SCOTT H MEYER RDRL WMP E M BURKINS

NO. OF COPIES	ORGANIZATION
	RDRL WMP F
	M CHOWDHURY
	A FRYDMAN
	N GNIAZDOWSKI
	R GUPTA
	RDRL WMP G
	N ELDREDGE
	D KOOKER
	S KUKUCK
	G R PEHRSON

NO. OF COPIES	ORGANIZATION